

СЕКЦИЯ 2
РАДИАЦИОННЫЕ ЭФФЕКТЫ В ТВЕРДОМ ТЕЛЕ

SECTION 2
RADIATION EFFECTS IN SOLIDS

NON-DESTRUCTIVE CRYSTAL ROTATION BY SHI IMPACTS

Jacques O'Connell, Danielle Douglas-Henry
CHRTEM, University Way, Summerstrand, Port Elizabeth, South-Africa,
jacques.oconnell@gmail.com, s212244450@mandela.ac.za

We investigated the microstructure of single crystal NiO irradiated at 45° off-normal incidence by 593 MeV Au ions to a fluence of $1.4 \cdot 10^{14}$ ions/cm² using electron microscope based techniques. It was found that the surface 11 μm thick layer experienced significant rotation along the direction of the incident ion beam projected onto the specimen surface while SAED showed the specimen as a whole remains single crystalline. Rotation vs depth profiles obtained from EBSD, TKD and SAED agreed well and suggests a maximum rotation of about 25° from the original <001> surface normal which is in agreement with on-line XRD measurement performed during irradiation. STEM microstructural analysis showed a high density of dislocations decorating the boundaries of nm sized cells exhibiting slight orientation differences. It was concluded that radiation induced stress buildup leads to the creation of low energy dislocation networks surrounding cells with minor orientation differences. These orientation differences are driven in along a specific direction due to unbalanced shear stress resulting from off normal irradiation and the residual stress from each thermal spike.

Keywords: SHI; TEM; EBSD; TKD; XRD.

Introduction

Swift heavy ion (SHI) of energies exceeding 1 MeV/amu are known to produce unique damage morphologies when impacting susceptible materials. These defects range from individual point defects and color centers to well aligned amorphous cylinders along the ion trajectories. The main reason for this unique mode of damage production is the intense electronic excitation along the ion path with virtually no energy lost to nuclear collisions until the very end of ion range [1-3].

A relatively under investigated effect of off normal SHI irradiation is that of a reversible collective rotation of crystalline grains [4-5]. Unfortunately, since the analysis in this work was based on XRD, very little is known about the microstructure of the rotated material and the depth dependence of the rotation.

In this work we report on the use of electron microscopy based techniques to gain further insight into the microstructure of 593

MeV Au irradiated single crystal NiO. NiO falls into the group of so-called non-amorphizable materials w.r.t. SHI irradiation as it is extremely resistant to radiation induced amorphization even up to fluences resulting in multiply overlapped ion tracks. This makes it an ideal candidate for microstructural analysis using electron diffraction based techniques as used in this work.

Experimental

Single crystal NiO (MaTeck) with <001> surface normal was irradiated at 45° off-normal incidence with 593 MeV Au ions at the former ISL lab in Berlin to a fluence of 1.4×10^{14} ions/cm². Specimens for electron backscatter diffraction (EBSD) were prepared by ion beam cross sectional polishing using 6 keV Ar ions in a JEOL SM-09020CP polisher. Specimens for transmission electron microscopy (TEM) were prepared by standard focused ion beam (FIB) lift-out technique using an FEI Helios 650 dual beam system and the resulting lamellae

were analyzed in a JEOL ARM200F analytical TEM operating at 200 kV. EBSD and transmission Kikuchi diffraction (TKD) was performed using an Oxford Instruments (HKL) Nordlys detector mounted on a JEOL JSM7001F scanning electron microscope (SEM).

Results

Figure 1 shows the relevant crystallographic axes and irradiation direction relative to the cross sectionally polished (denoted CP) surface of the specimen where EBSD data was collected. The orange arrow on the surface of the crystal represents the ion direction along a $\langle 011 \rangle$ crystal axis. The yellow arrow about the $\langle 001 \rangle$ axis pointing out of the page denotes the direction of observed crystal rotation due to irradiation.

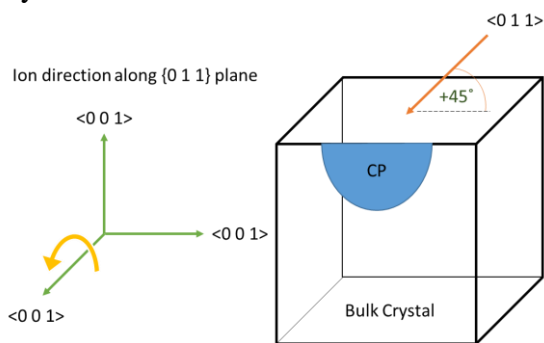


Fig. 1. Irradiation geometry

Figure 2 shows a bright field (BF) and annular dark field (ADF) STEM image pair of the irradiated material viewed along the ion direction. Dark spots visible in the BF image are ion tracks viewed edge-on. The brighter regions (more clearly visible in the ADF image) represent areas of slightly differing crystal orientation. These cells of subtle orientation difference are formed because of uncompensated shear stress buildup during irradiation. The dislocations present at the cell boundaries show up as slightly brighter lines surrounding the cells. However, the inset selected area electron diffraction (SAED) pattern shows that these misorientations are extremely small and the material remains effectively single crystal.

Figure 3 shows a plot of relative crystal orientation as a function of depth below the

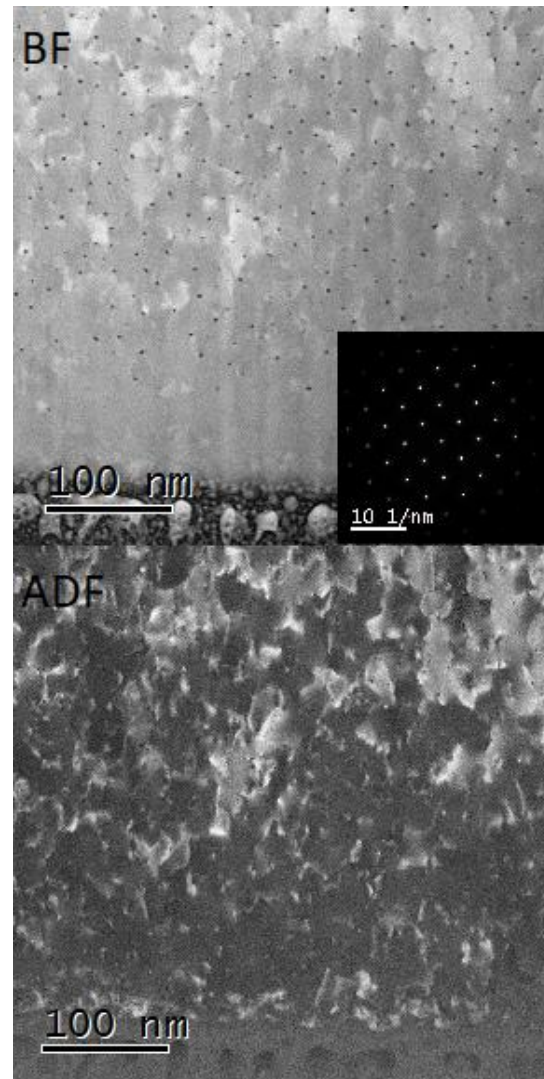


Fig. 2. BF/ADF STEM pair in a plane normal to the ion direction

irradiated surface as measured by EBSD, TKD and SAED. TKD and SAED was performed on the same lamella while EBSD was performed on the bulk crystal from which the lamella was extracted. Due to the rough unpolished surface of the specimen, data could not reliably be collected within the first 2-3 μm .

Discussion

Stress buildup due to repeated ion impacts and associated thermal spikes leads to the development of a dense dislocation network bounding cells of relatively low dislocation density. Uncompensated shear stress produced by the off normal incident ions leads to slip along these cell boundaries

causing minor orientation differences between adjacent cells, but over large distances produce a relatively uniform rotation of the bulk crystal. This is evident from the relatively flat contrast within dislocation bounded cells in figure 2 together with the rotation vs depth plots in figure 3.

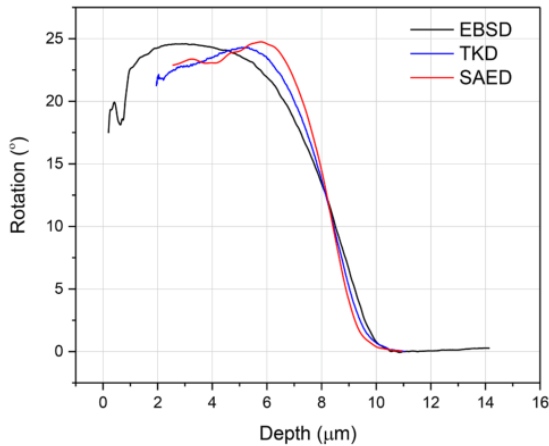


Fig. 3. Depth dependent crystal rotation curves obtained from three complimentary techniques

The areal density of visible ion tracks in figure 2 is significantly lower (400 times lower) than the ion fluence. This behavior is consistent with that of other non amorphizable materials such as Al_2O_3 [6] where a steady state of track density develops when the rate of creation of new ion tracks matches that of ion induced annealing of existent tracks. Crystal rotation extends to a depth of about $11 \mu\text{m}$ and reaches a peak relative rotation of about 25° within $3 \mu\text{m}$ of the onset of rotation. Relative rotation appears to reach a steady state between the surface and this depth although large uncertainties in the first few μm due to a rough unpolished surface prevents extracting reliable dynamics from these curves. Good agreement between the curves generated by complimentary techniques as well as agreement with maximum rotation angle derived from on-line XRD measurement (26°) proves that all of the employed techniques may be considered suitable for obtaining depth dependent rotation curves. However due to simpler specimen preparation and higher data throughput, we conclude that EBSD is the preferable technique in this case. Because EBSD does

not require specimen thinning to electron transparency, it further minimizes the risk of stress relaxation in the specimen due to thinning.

Conclusions

We successfully performed local crystal orientation mapping as a function of depth below the irradiated surface for SHI irradiated NiO using EBSD, TKD and SAED. Good agreement was found between techniques and results were comparable to that of on line XRD performed during the irradiation session. We conclude that for specimen preparation and data throughput reasons, EBSD is the preferable technique for future work. STEM and SAED analysis revealed an almost continuous single crystal structure interrupted by a dense network of dislocations separating cells of slight orientation differences which add up to facilitate the observed macroscopic rotation.

The authors would like to acknowledge Siegfried Klaumuenzer for the NiO specimens and fruitful discussion.

References

1. Bouffard S., Gervais B., Leroy C. Basic phenomena induced by swift heavy ions in polymers. *Nucl. Inst. Methods Phys. Res. B.* 1995; 105(1-4): 1-4.
2. Chen C., Pang L.L., Lu Q., Wang L., Tan Y., Wang Z. et al. Refractive index engineering through swift heavy ion irradiation of LiNbO₃ crystal towards improved light guidance. *Sci. Rep.* 2017; 7(10805): 1-7.
3. Toulemonde M., Bouffard S., Studer F. Swift heavy ions in insulating and conducting oxides: tracks and physical properties. *Nucl. Inst. Methods Phys. Res. B.* 1994; 91(1-4): 108-123.
4. Zizak I., Schumacher G., Darowski N., Klaumünzer S. Ion-Beam-Induced Collective Rotation of Nanocrystals. *Phys. Rev. Lett.* 2008; 101(065503): 1-4.
5. Zizak I., Darowski N., Klaumünzer S., Schumacher G., Gerlach J.W., Assmann W. Grain rotation in nanocrystalline layers under influence of swift heavy ions. *Nucl. Inst. Methods Phys. Res. B.* 2009; 267(6): 944-948.
6. O'Connell J.H., Rymzhanov R.A., Skuratov V.A., Volkov A.E., Kirilkin N.S. Latent tracks and associated strain in Al_2O_3 irradiated with swift heavy ions. *Nucl. Inst. Methods Phys. Res. B.* 2016; 374: 97-101.